Sequences, Structural Models, and Cellular Localization of the Actin-related Proteins Arp2 and Arp3 from *Acanthamoeba*

Joseph F. Kelleher, Simon J. Atkinson, and Thomas D. Pollard

Department of Cell Biology and Anatomy, Johns Hopkins Medical School, Baltimore, Maryland 21205

Abstract. We cloned and sequenced the two actin-related proteins (Arps) present in the profilin-binding complex of *Acanthamoeba* (Machesky, L.M., S. J. Atkinson, C. Ampe, J. Vandekerckhove, and T. D. Pollard. 1994. *J. Cell Biol.* 127:107–115). The sequence of Arp2 is more similar to other Arp2s than to actin, while the sequence of Arp3 is more similar to other Arp3s than to actin. Phylogenetic analysis of all known Arps demonstrates that most group into three major families, which are likely to be shared across all eukaryotic phyla. Together with conventional actins, the Arps form a larger family distinct from structurally related ATPases such as Hsp70's and sugar kinases. Atomic models of the Arps based on their sequences and the structure of actin provide some clues about function. Both Arps have atoms appropriately placed to bind ATP and divalent cation. Arp2, but not Arp3, has a conserved profilin-binding site. Neither Arp has the residues required to copolymerize with actin, but an Arp heterodimer present in the profilin-binding complex might serve as a pointed end nucleus for actin polymerization. Both *Acanthamoeba* Arps are soluble in cell homogenates, and both are concentrated in the cortex of *Acanthamoeba*. The cellular concentrations are 1.9 μM Arp2 and 5.1 μM Arp3, substoichiometric to actin (200 μM) but comparable to many actin-binding proteins.

THE actin-related proteins actin-related protein (Arp)[1]2 and Arp3 are conserved across eukaryotic phyla and are essential for yeast, but very little is known about their molecular interactions and functions. One clue is that they are present in equimolar amounts with several other proteins in a complex of proteins from *Acanthamoeba castellanii* (Machesky et al., 1994) that binds to profilin. Profilin also binds polyphosphoinositides, poly-L-proline, and actin (for a review see Machesky and Pollard, 1993) and has multiple effects on actin polymerization (for a review see Theriot and Mitchison, 1993). As these molecules seem to play some vital role, characterization of the Arps present in the *Acanthamoeba* complex may provide general principles applicable to all eukaryotes.

Actin-related proteins are broadly defined as proteins sharing significant (30–60%) amino acid identity with conventional actin isoforms, but not enough to be considered conventional actins, which are among the most highly conserved of known proteins (Hightower and Meagher, 1986). To date, genetic and molecular genetic studies have revealed three large classes of Arps as well as several outliers that may be founding members of other ubiquitous families (Frankel et al., 1994; Fyrberg et al., 1994; Harata et al., 1994).

The Arp1 class is the best characterized (for reviews see Clark and Meyer, 1993; Schroer, 1994). Arp1, also referred to as centractin, is a component of a multi-protein assembly that promotes dynein-based vesicle motility (Lees-Miller et al., 1992*a*; Paschal et al., 1993) and may be associated with centrosomes (Clark and Meyer, 1992). Arp1 binds nucleotide, cocycles with polymerized actin (Melki et al., 1993), and forms a short filament resembling filamentous actin in the dynactin complex (Schafer et al., 1994). *S. cerevisiae* Arp1 null mutants have defects similar to dynein mutants; mitotic spindle orientation and nuclear migration are impaired (Clark and Meyer, 1994; Muhua et al., 1994). Nuclear distribution is defective in *N. crassa* with a variety of Arp1 mutations (Plamann et al., 1994). Arp1 is present in *C. elegans* (Waterston et al., 1992) and *D. melanogaster* (Fyrberg et al., 1994) and humans have two closely related isoforms (Clark et al., 1994).

Genes encoding Arp2 and Arp3 were discovered in yeast. The *S. cerevisiae* ACT2 gene encodes a 44-kD protein now called Arp2 with 47% amino acid identity to vertebrate skeletal muscle α-actin (Schwob and Martin, 1992). Null mutations are lethal. Since the cells arrested as a single cell with a large bud, the authors postulated a role of ACT2p in cell division or cytokinesis (Schwob and Mar-

Please address all correspondence to J. F. Kelleher, Department of Cell Biology and Anatomy, Johns Hopkins Medical School, 725 North Wolfe Street, Baltimore, MD 21205. Tel.: (410) 955-5672. Fax: (410) 955-4129.

The current address of S. J. Atkinson is the Department of Medicine-Nephrology, Indiana University School of Medicine, Fesler Hall 115, 1120 South Drive, Indianapolis, IN 46202.

1. *Abbreviation used in this paper*: Arp, actin-related protein.

tin, 1992). The *S. pombe* act2 gene, also essential, encodes a 47.4-kD protein now called Arp3 with 35–40% amino acid identity to conventional actin (Lees-Miller et al., 1992*b*). The sequences of these two yeast Arps are as different from each other as each is from actin. Genes encoding homologues of each Arp are found in *C. elegans* (Waterston et al., 1992), *D. discoideum* (Murgia et al., 1995; Atkinson, S. J., unpublished), *D. melanogaster* (Fyrberg et al., 1994), *G. gallus* (Michaille et al., 1995), and *B. taurus* (Tanaka et al., 1992). *Acanthamoeba* Arp2 and Arp3 are present in a complex of proteins isolated by affinity chromatography on profilin-agarose (Machesky et al., 1994).

To learn more about the structures and functions of Arp2 and Arp3 ,we have cloned and sequenced cDNAs for both from *Acanthamoeba.* We analyzed the phylogenetic relationships of all known Arps, built structural models of Arp2 and Arp3 to establish their potential for interactions with each other and other proteins, and determined their cellular concentrations and distributions.

Materials and Methods

cDNA Cloning and Sequencing

We used the Pileup program in the GCG version 6.0 (Genetics Computer Group, University of Wisconsin, Madison, WI) analysis package to align the sequences of *Acanthamoeba* actin (Genbank accession number V00002), vertebrate skeletal muscle α-actin (J00805), human actin-RPV (Z14978), *S. cerevisiae* ACT2p (X61502), and *S. pombe* act2p (M81068). We chose regions of homology and designed oligonucleotides for amplification of actin-related DNAs from *Acanthamoeba* genomic DNA by degenerate oligonucleotide PCR (Sambrook et al., 1989). Reaction products included a 450-bp DNA that was predicted to encode partially a homologue of *S. cerevisiae* ACT2. We used this fragment to screen by hybridization an *Acanthamoeba* cDNA library constructed from poly-A+ RNA in Lambda Zap II (Zap-cDNA synthesis kit, Stratagene, La Jolla, CA) using established procedures (Sambrook et al., 1989). We obtained a full-length cDNA encoding a 44-kD Arp2. We obtained a full-length cDNA clone encoding a 48.6-kD Arp3 using a 54-mer synthetic oligonucleotide based on the sequence of the 47 k p22 peptide (Machesky et al., 1994) to screen the *Acanthamoeba* cDNA library.

We sequenced both strands of the cDNA clones using U.S. Biochemical Company (Cleveland, OH) Sequenase 2.0 reagents and protocols with successive synthetic oligonucleotide primers. Annealing reactions included 0.05 μg/μl single strand–binding protein (U.S. Biochemical Company) to reduce secondary structure artifacts. [^{35}S]dATP was purchased from Dupont/New England Nuclear (Boston, MA).

Phylogenetic Analysis

Actin and Arp sequences were retrieved from Genbank and EMBL databases. Names and accession numbers or references are as follows: *S. pombe* act2p, M81068; *D. discoideum* 49-kD actin-related protein (Genbank accession number Z46418 and Atkinson, S. J., unpublished observation); *A. castellanii* Arp3, U29610; *C. elegans* ACTD, (Waterston et al., 1992); bovine actin2, D12816; *D. melanogaster* Arp66B, X71789; *S. cerevisiae* ACT5p (X79811); *N. crassa* centractin, L31505; *P. carinii* actin II, L21184; *C. elegans* ActB (Waterston et al., 1992); *D. melanogaster* Arp87C, X78488; human α-Arp1, Z14978 (human and canine centractin, S45367, are identical); human β-Arp1, X82207; *S. cerevisiae* ACT1p, V01288; *S. pombe* act1p, Y00447; *Acanthamoeba* actin, V00002; *G. gallus* ACTL, X73971; *D. melanogaster* Arp79B, M18829 and J01064; *C. elegans* actin gene (1), X16796; vertebrate skeletal muscle α-actin, J00805, K02172, and 022577; *D. melanogaster* Arp53D, X78487; *D. melanogaster* Arp14D, X78486; *C. elegans* ActC, (Waterston et al., 1992); *D. discoideum* 44-kD Arp (Atkinson, S. J., unpublished observation); *A. castellanii* Arp2, U29609; *S. cerevisiae* ACT2p, X61502; *D. melanogaster* Arp13E, L25314.

We used the program CLUSTAL V (Higgins et al., 1992) to create a multiple alignment of these sequences. For maximum parsimony analysis, the PHYLIP program SEQBOOT was used to create a bootstrapped data set (Felsenstein, 1985) of 50 random resamplings of the original data set from the CLUSTAL V alignment. The PHYLIP parsimony program PROTPARS was used to search for the most parsimonious tree from each random resampling, with five rounds of random order entry per data set to minimize loading order artifacts. The PHYLIP program CONSENSE was used to calculate the strict majority rule consensus tree from the output of the PROTPARS run.

Bootstrapped distance matrix analysis was performed using CLUSTAL V with 100 bootstrap trials. This program uses the neighbor joining method of Saitoh and Nei (1987). 1,000 trials gave identical topologies and very similar statistics. Sequences conforming to a motif determined from alignment of the three dimensional structures of actin, hexokinase, and Hsc70 (Bork et al., 1992) were used to find homologous regions in the Arps. Bootstrapped distance matrix analysis as above was performed on the five part sequence pattern of this ATPase domain.

Structural Model Building

Three dimensional models of *Acanthamoeba* Arp2 and Arp3 were computed beginning with the aligned sequences and the coordinates of the corresponding residues of vertebrate skeletal α actin, PDB accession number 1ATN (Kabsch et al., 1990). Models were built interactively in the program CHAIN running on a Silicon Graphics IRIS workstation. Residues differing between actin and either Arp in the alignment were changed with the REPLACE or MUTATE commands. Side chain conformations were selected from a rotomer library to avoid obvious steric clashes. Insertions relative to actin were placed with the INSERT command at positions based upon the CLUSTAL alignment and modeled as loops. The CHAIN subroutine REGULARIZE was used to optimize bond lengths and angles in local regions after alteration. Initial structures were energy minimized with the program X-PLOR (Brünger, 1992) using 120 iterations of the MINIMIZE POWELL routine. Figures were generated from coordinates using the programs MOLSCRIPT (Kraulis, 1991) or SETOR (Evans, 1993).

Recombinant Protein Expression

We engineered full-length cDNAs encoding Arp2 and Arp3 into the T7-based expression vector pMW172 (Way et al., 1990) for expression in BL21(DE3) *E. coli.* The bacteria sequestered the expressed proteins in inclusion bodies. We isolated inclusion bodies (Nagai and Thøgersen, 1987) and solubilized recombinant protein with 8 M urea in 20 mM Tris-HCl (pH 8) containing 20 mM 2-mercaptoethanol.

Antibody Preparation and Purification

We raised antibodies to recombinant Arp2 and Arp3 in New Zealand white rabbits (Bunnyville Farms, Littletown, PA) as described (Fujiwara and Pollard, 1976), immunizing at sites along the back. We immunized rabbit JH-46 with an SDS-PAGE gel band (Machesky et al., 1994) of rArp2 and boosted with partially purified rArp2 solubilized from inclusion bodies and dialyzed against H_2O. We immunized and boosted rabbit JH-47 with partially purified rArp3. We purified crude polyclonal antisera by incubation with either rArp2 or rArp3 on immunoblot strips (Pollard, 1984). Preimmune antiserum was mock purified using blot strips identical to those used for immune antiserum.

Immunofluorescence

Acanthamoeba were maintained and fixed as in Yonemura and Pollard (1992). Cells were fixed in 1% formaldehyde in methanol for 5 min at −20°C, rehydrated in PBS (0.15 M NaCl, 0.01% NaN_3, 10 mM sodium phosphate, pH 7.4) and incubated for 15 min in 1% BSA (bovine serum albumin, Sigma Chem. Co., St. Louis, MO) in PBS to block nonspecific binding. We incubated cells with affinity purified primary antiserum in 1% BSA in PBS for 1 h and washed in 1 % BSA in PBS for 15 min. Preabsorbed (Yonemura and Pollard, 1992) rhodamine-conjugated goat anti–rabbit IgG secondary antibody (Molecular Probes, Eugene, OR) was applied for 30 min. Double staining for filamentous actin and Arp2 was accomplished by simultaneous incubation with secondary antibodies and BODIPY-FL phallicidin (Molecular Probes). Cells were washed in 1% BSA in PBS for 15 min and mounted in 50% glycerol containing 20 mM DTT and 5.6 mM *p*-phenylenediamine. We observed and photographed labeled cells using both phase contrast and fluorescence microscopy as described previously (Fujiwara and Pollard, 1976).

Gel Electrophoresis and Immunoblots

Log phase cells from liquid culture were washed once in 50 mM NaCl and homogenized in a Dounce homogenizer at 0°C in 3 vol of sucrose extraction buffer (10% sucrose, 20 mM imidazole-HCl, pH 7.5, 1 mM ATP, 1 mM EGTA, 1 mM DTT, 0.1 mM PMSF, and 1 μg/ml each of clostripain, leupeptin, pepstatin A, benzamidine, and soy trypsin inhibitor). Lysis was monitored by observation with phase contrast microscopy and typically required 40 passes. These homogenates were fractionated by successive centrifugation at 4°C at 6,100 *g*, 9,200 *g*, and 100,000 *g*. Samples of the homogenate and each supernatant fraction were added to 4 vol boiling SDS sample buffer (Laemmli, 1970), boiled 2 min and immediately frozen in liquid nitrogen. At the time of electrophoresis, samples were boiled for 2 min.

Polypeptides were separated by SDS-PAGE (Laemmli, 1970), transferred to nitrocellulose and reacted with antibodies (Towbin et al., 1979) using high stringency wash conditions (2 M urea, 100 mM glycine 1% Triton X-100). Bound antibodies were detected with [^{125}I]protein A and autoradiography or by chemiluminescence (Amersham Corp., Arlington Heights, IL).

Quantitation

Concentrations of purified rARPs were determined by comparison with rabbit skeletal muscle actin standards on gels stained with Coomassie blue and digitized using Collage software (Fotodyne, New Berlin, WI) on a Macintosh computer. The concentration of Arps in homogenates was determined on immunoblots by comparison of homogenates with a dilution series of rArp2 or rArp3. Proteins were transferred to nitrocellulose membranes and reacted with specific antibodies, followed by washing and detection of bound antibodies using freshly prepared [^{125}I]protein A (kind gift of W. C. Earnshaw). The intensities of the Arp2 and Arp3 bands in the homogenate were compared with the standards by densitometry of autoradiograms. The concentration of Arp2 and Arp3 in *Acanthamoeba* was calculated assuming that one gram of pelleted amoebas occupies one milliliter.

Results

Comparison of Arp Sequences

We obtained a full-length *Acanthamoeba* cDNA clone encoding a 388–amino acid protein with a predicted mass of 44 kD. The protein contains peptide sequences found by Machesky et al. (1994) in a 44-kD actin-related protein present in a profilin-binding complex. This protein sequence is 50% identical (69% similar) to both *Acanthamoeba* actin and vertebrate skeletal muscle α actin. The predicted isoelectric point is 7.6. Those of *Acanthamoeba* actin and vertebrate skeletal alpha actin are 5.4 and 5.2. This 44-kD protein shows higher homology to members of the Arp2 family (Muhua et al., 1994; Schroer et al., 1994) than to actins or other Arps, so we named it *Acanthamoeba* Arp2. It is 66% identical (77% similar) to *S. cerevisiae* ACT2, 68% identical (82% similar) to *C. elegans* ActC, and 69% identical (84% similar) to *D. melanogaster* Arp14D.

Using a degenerate oligonucleotide based upon a peptide sequence from an *Acanthamoeba* Arp (Machesky et al., 1994), we obtained a full-length *Acanthamoeba* cDNA clone encoding a 427–amino acid protein of 48.6 kD with a predicted isoelectric point of 7.0. This sequence is 38% identical (61% similar) to both *Acanthamoeba* actin and vertebrate skeletal muscle α actin, but more homologous to several members of the Arp3 family (Muhua et al., 1994; Schroer et al., 1994), so we have named the protein *Acanthamoeba* Arp3. It is 63% identical (78% similar) to *S. pombe* act2, 66% identical (78% similar) to *C. elegans* ActD, and 71% identical (81% similar) to both bovine actin 2 and *D. melanogaster* Arp66B.

Both cDNAs have a high frequency of G or C in the third position of codons. This is similar to other *Acanthamoeba* genes, which also show a high G/C codon bias (Hammer et al., 1987).

Sequence-based phylogenetic analysis using bootstrapped distance matrix methods groups conventional actins in one family, with Arp sequences from a wide spectrum of eukaryotes clustered in three other families (Fig. 2 *A*). Bootstrapped maximum parsimony analysis gives a tree with identical topology (not shown). The Arp1 family is the closest to actin, the Arp2 family is next, and the Arp3 family is the most divergent of the major families. Several Arps do not fall into any of these groups. *D. melanogaster* Arp53D is more closely related to the conventional actins than any of the other Arps, but is different enough to be excluded from the actin family. *D. melano-*

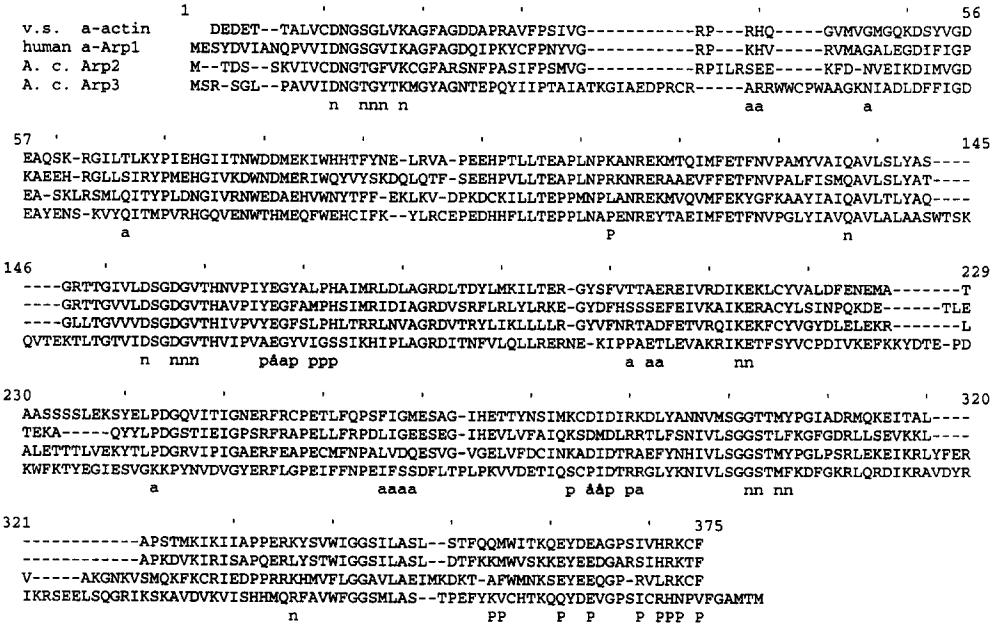

Figure 1. Alignment of translated *Acanthamoeba* Arp2 and Arp3 cDNA sequences with vertebrate skeletal muscle α-actin and human α-Arp1. Numbers refer to actin, with tick marks every 10 residues. Letters below the alignment mark the following: *n*, nucleotide binding; *a*, actin subunit contacts in the Lorenz et al. (1993) model of filamentous actin; *P*, profilin contacts in subdomain 1; *p*, profilin contacts in subdomain 3; *å*, both actin and subdomain 1 profilin contacts. The cDNA sequences are available from GenBank/EMBL/DDBJ under accession number U29609 (Arp2) and U29610 (Arp3).

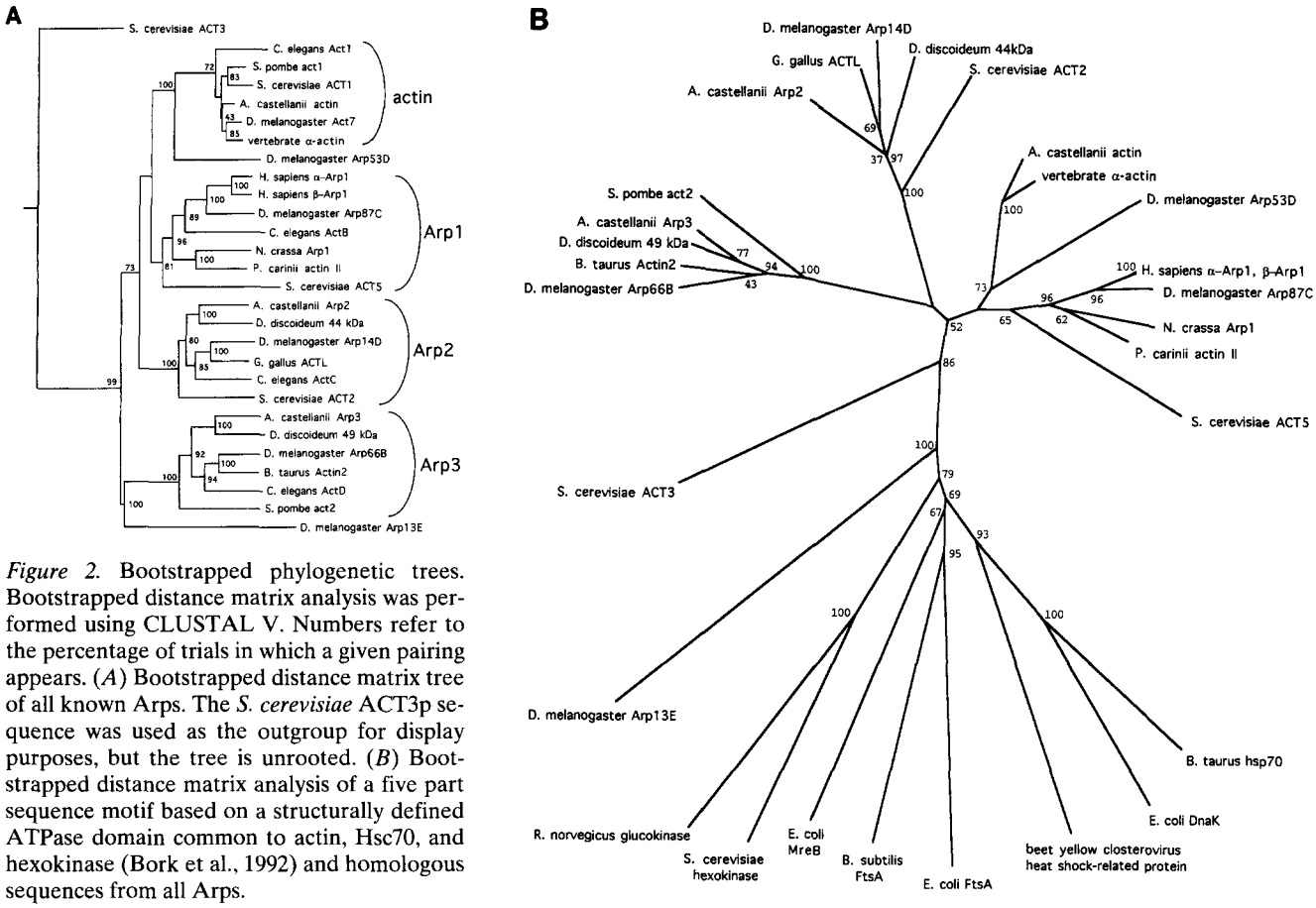

Figure 2. Bootstrapped phylogenetic trees. Bootstrapped distance matrix analysis was performed using CLUSTAL V. Numbers refer to the percentage of trials in which a given pairing appears. (*A*) Bootstrapped distance matrix tree of all known Arps. The *S. cerevisiae* ACT3p sequence was used as the outgroup for display purposes, but the tree is unrooted. (*B*) Bootstrapped distance matrix analysis of a five part sequence motif based on a structurally defined ATPase domain common to actin, Hsc70, and hexokinase (Bork et al., 1992) and homologous sequences from all Arps.

gaster Arp13E and *S. cerevisiae* ACT3p are the most divergent Arps, falling far from the other groups.

Phylogenetic analysis of a five part sequence motif describing a shared ATPase domain determined from optimal alignment of the three dimensional structures of actin, Hsc70, and hexokinase (Bork et al., 1992) groups the three major Arp families together with actin in a cluster with a common root. This group then joins all other sequences sharing this motif at approximately the same distance (Fig. 2 *B*). *D. melanogaster* Arp13E falls far from all other Arps in this analysis and may not be an Arp at all. Distances between the common root of the actin/Arp superfamily and many of the other sequences in the tree, as well as distances between sequences at the bottom of the tree are very likely gross underestimates due to multiple mutations at single positions not being taken into account in the analysis. A variation of this distance matrix method developed by Kimura (1983) which accounts for multiple substitutions through evolution predicts much larger values, with many values reported as infinite (not shown). The absolute topology of the lower part of the tree must therefore be regarded as approximate.

Atomic Models of Arp2 and Arp3

Our model of *Acanthamoeba* Arp2 (Fig. 4 *A*) is based upon alignment of its primary sequence with that of vertebrate skeletal α actin (Fig. 1), superimposition of this alignment on the three dimensional structure of actin (Fig. 3 *A*) (Kabsch et al., 1990), and energy minimization using the program X-PLOR (Brünger, 1992). After this refinement the rms deviation of the backbone of the Arp2 model from actin was only 0.55 Å except for one major and one minor insertion (Fig. 4 *A*). For simplicity, residue numbers given in Fig. 1 and the following descriptions are those in the actin sequence but refer to homologous residues in the model structures. Eleven amino acids are inserted in the loop between amino acids 320 and 328 in the actin structure. Two amino acids are inserted in the DNAse I binding loop, between residues 38 and 39.

We built and refined our model of *Acanthamoeba* Arp3 (Fig. 4 *B*) in the same way as the Arp2 model. It contains a number of insertions relative to actin, but the rms deviation of the backbone of the other residues from actin is only 0.24 Å. Three of the insertions can be accommodated in loops at the surface of the protein. Fourteen amino acids are inserted between residues 42 and 43 in the DNAse I binding loop, eight amino acids are inserted in the loop between residues 145 and 150, and sixteen amino acids are inserted in the loop connecting amino acids 320 and 328 in subdomain three. An extra six residues are present at the carboxyl terminus of Arp3. Six amino acids were inserted between residues 231 and 232 in a turn connecting α helix 7 with β strand 13 in subdomain four. Although the regions flanking actin residues 227 to 250 are homologous between actin and Arp3, within this region none of the 30

residues of Arp3 are identical to the 24 actin residues. The insertion in the Arp3 structure could have been placed in a number of locations in this interval, but the turn between residues 230 and 238 was chosen to minimize disruption of the overall structure.

Insertions in Arp2 and Arp3 relative to actin were modeled as extended loops. Energy minimization constrained these loops to occupy allowed peptide backbone geometries, but they are otherwise unconstrained by any data. We have no basis for imposing any particular structure on these regions in the models, so we chose this simple representation to convey where the extra residues are in space.

The three dimensional distribution of conserved and nonconserved (with respect to actin) residues within the hydrophobic core of each Arp seems random, with approximately the same overall ratio of conserved to nonconserved residues as the entire protein. Arp2 is 50% identical to actin; residues in the hydrophobic core of Arp2 are ~50% conserved. Arp3 is 38% identical to actin; residues in the hydrophobic core are ~40% conserved.

In contrast, conserved amino acids occur in clusters on the surfaces of Arp2 and Arp3; the Arps display subsets of the three dimensional surface features present in actin. Consistent with their overall levels of conservation, Arp2 has more actin-like surface patches than Arp3. Arp2 has clusters of conserved residues on surface faces of α helices and β sheets in subdomains 1 and 2, in loops at both the barbed and pointed ends and along the back face of the molecule (Fig. 4 *C*). In Arp3, there is one large conserved face on the right side of subdomain 1 in the standard view and several smaller clusters of conserved residues at the barbed end and along the back face of the molecule (Fig. 4 *D*).

Nucleotide Binding

Residues which bind nucleotide in the cleft of actin (Figs. 3 *A* and 5 *A*) are present in similar three dimensional arrangements in both Arp2 and Arp3 (Fig. 5). The pocket surrounding the adenosine base is conserved. T303 is replaced in both structures by a serine which fits well within the space available. Y306 and K336 are conservatively replaced in Arp3 by phenylalanine and arginine, respectively. The atoms which hydrogen bond with the ribose hydroxyls and the phosphates of ATP are conserved, with eight identical contacts and two substitutions. Threonine replaces S14 in both Arps and maintains similar contacts with the gamma phosphate of ATP. Actin L16 is replaced by phenylalanine in Arp2 and by tyrosine in Arp3, but the side chain fits within the structure in each case and points away from the nucleotide binding site, while the backbone NH remains in position to ligate the beta phosphate of ATP.

Profilin Binding

A comparison (Fig. 3, *D* and *E*; Fig. 4, *C* and *D*) of the actin residues in contact with profilin in cocrystals (Schutt et al., 1993) with the Arp models suggests that Arp2 but not Arp3 binds profilin. These residues are located at the base of subdomains 1 and 3 (Fig. 3, *D* and *E*). In Arp2 (Fig. 4 *C*), ten of the eleven subdomain three contact residues are identical, and one is conservatively substituted (Y169F). Five of the ten contact residues in subdomain 1 are identical in Arp2. The substitution of side chain contact K113L does not create an obvious steric problem, but a favorable charge interaction with E82 of profilin is lost. Two other replaced side chain contacts may be favorable; M355F may place the substituted phenylalanine ring in position to interact with the ring of H119 of profilin, while the side chain of I369R may fold to create an electrostatic interaction with E129 of profilin while minimizing steric problems. The remaining Arp2 substitutions, Q354A and H371L, are for residues making primarily backbone contacts with profilin; no side chain steric clash is evident for either. In Arp3 (Fig. 4 *D*), five of the eleven subdomain 3 contacts are identical while one is conservatively substituted for L171I. Several substitutions change interacting side chains but do not create steric problems; P172G may be accomodated, Y166A lacks several favorable hydrophobic interactions and H173S fits but lacks a favorable interaction with F59 of profilin. K284S is a backbone contact with no steric problems from substitution. It is unclear if D286P creates steric clashes. Only two of ten subdomain 1 contact residues are present in Arp3 and two are conservatively substituted for. No obvious steric problems arise from the remaining substitutions, although several favorable interactions with profilin are lost. The presence of six additional COOH-terminal amino acids in Arp3 vs actin may cause significant steric clashes with profilin. Due to this insertion, major rearrangements of both profilin and Arp3 would be necessary to allow contacts similar to those in the profilin:actin-binding site.

Actin Polymerization

Examination of the residues in each Arp corresponding to those making contact between actin subunits in the Lorenz et al. (1993) model of filamentous actin provides valuable clues about the capacity of the Arps to assemble. Along the two start actin filament helix residues at the pointed end of one actin subunit, at the top of subdomains 2 and 4 (in the standard view shown in Fig. 3), interact with residues at the barbed end of a second subunit at the bottom of subdomains 1 and 3. Residues predicted to make contacts between subunits in the Lorenz et al. (1993) model are depicted in black in the Van der Waals representations of actin in Fig. 3, *B* and *C* to allow comparisons with the Arp models in Fig. 4, *C* and *D*. Although both Arp2 and Arp 3 have insertions in the loop between 320 and 328 at the bottom of subdomain 3, these extra residues would not preclude interaction with the pointed end of an actin subunit in a filament.

Many residues that are in contact along the 2 start helix are conserved at the barbed (286-288, I289T, 166-169, 375) and pointed (203-204, E205D, 243-245) ends of Arp2. However, the pointed end substitution T202R may sterically interfere with both the backbone and side chain of D286 at the barbed end of an adjacent actin subunit and preclude polymerization. The Arp2 barbed end substitution K291A does not create a steric clash but lacks a potential H-bond to an adjacent subunit.

Many of the side chain contacts along the 2 start actin filament helix are conserved at the barbed end of Arp3 but none is conserved at the pointed end. At the barbed end residues 287-288 and 167-169 are identical. The substitu-

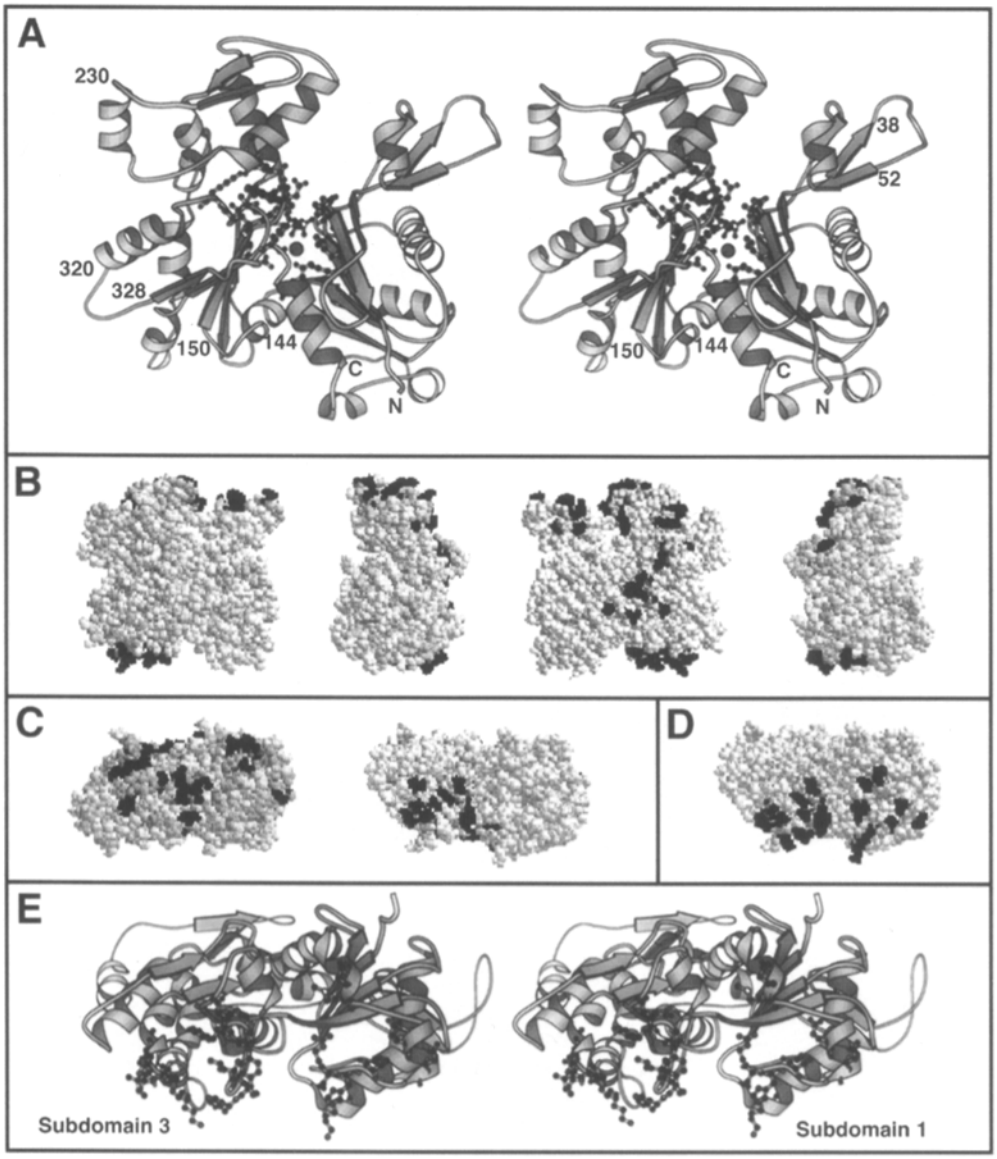

Figure 3. Stereo pair ribbon diagram (*A* and *E*) and Van der Waals surface representations (*B, C,* and *D*) of three dimensional crystal structure of rabbit skeletal muscle α-actin (Kabsch et al., 1990). (*A*) Actin with nucleotide-binding site in ball and stick representation to orient Fig. 5. (*B*) Actin with residues making contacts between subunits in the Lorenz et al. (1993) model of the actin filament shown in black. Images are successive ninety degree rotations showing, from left to right, front (view in *A*), right side, back, and left side of molecule. (*C*) Pointed end (*left*) and barbed end views with residues shaded as in *B*. (*D*) Barbed end view with residues contacting profilin in black. (*E*) Barbed end view with residues contacting profilin as balls and sticks.

tions I289T and K291R are conservative. The two nonconservative substitutions D286P and Y166A do not preclude binding to the pointed end of an adjacent subunit although D286P may create a minor steric problem with T202 of the next actin subunit. The six additional COOH-terminal amino acids in Arp3 may not interfere sterically with its ability to make barbed end contacts like those present in the 2 start actin filament helix. In contrast, all of the subunit–subunit contact residues at the pointed end of Arp3 differ from actin. P243K and A204E could create significant steric clashes with many residues at the barbed end of an adjacent actin subunit and interfere with polymerization.

The major interaction along the actin filament genetic helix in the Lorentz et al. (1993) model features a three-bodied contact in which a loop of hydrophobic residues (F266, I267, G268, and M269) from one actin subunit inserts into a hydrophobic pocket formed by residues in subdomain 3 of a second subunit (Y166 and Y169) and subdomain 2 of a third subunit (I64, T66 and P38) across the genetic helix. The postulated loop would be LVDQ in Arp2 and IFSS in Arp3. The subdomain 3 residues are conserved in both Arps. P38K in Arp3 and T66Q in both Arps may cause steric problems at the subdomain 2 contact.

In the Lorenz et al. (1993) model, other interactions along the genetic helix occur between residues 110-112 and 176, 177 and 179 of one subunit and residues 191, 195-197, 199, 201 and 206 of a second subunit. These residues were not predicted to form hydrogen bonds, but are within 10 Å of each other. Many of these residues are conserved in the Arps and the substitutions do not appear to create steric clashes.

Cellular Concentrations and Localization of Arp2 and Arp3

Rabbit polyclonal antisera against bacterially expressed *Acanthamoeba* Arp2 and Arp3 each reacts with single major bands on Western blots of whole *Acanthamoeba* lysate (Fig. 6, *A* and *B*; Fig. 7). Lower molecular weight species in the homogenate sample in Fig. 6 *A* are Arp2 break down products that accumulate over time or upon repeated boiling of the sample as the major band disappears.

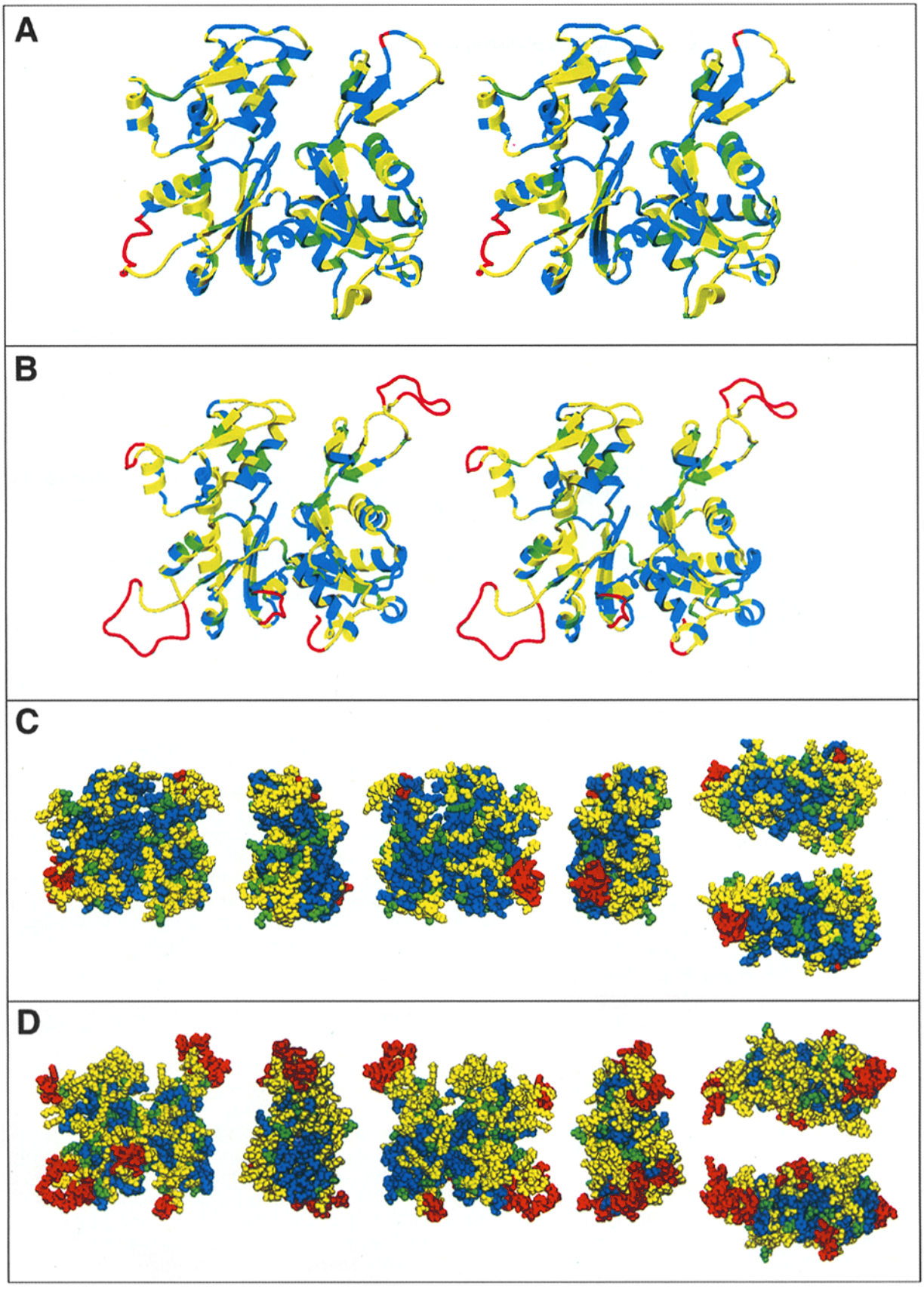

Figure 4. Ribbon diagrams (*A* and *B*) and Van der Waals surface representations (*C* and *D*) of model structures of *Acanthamoeba* Arp2 (*A* and *C*) and Arp3 (*B* and *D*). Images in *C* and *D* are successive ninety degree rotations showing, from left to right, standard view (as in *A* and *B*), right side, back, and left side of molecules. Pointed end (*top*) and barbed end (*bottom*) are depicted at far right. Color code: residues identical to actin are blue; conservative substitutions are green; non-conservative substitutions are yellow; and insertions are red.

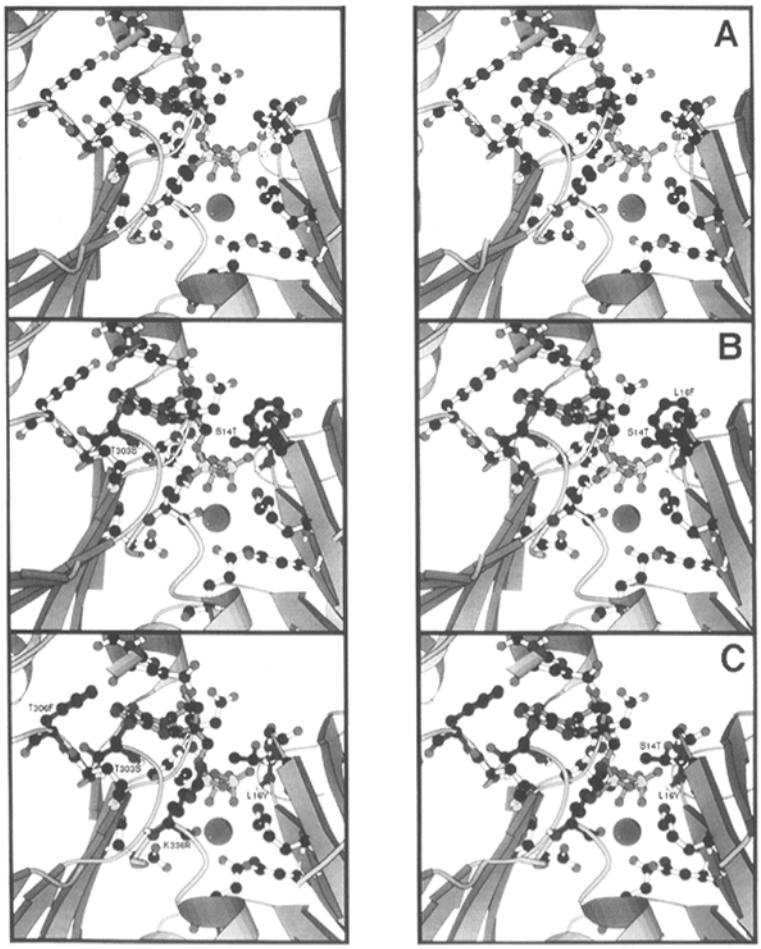

Figure 5. Stereo pairs of the nucleotide-binding site of actin and the Arp2 and Arp3 model structures viewed as in Fig. 3 *A*. ATP and calcium are docked into the model structures using the ATP and Ca^{2+} coordinates from the actin crystal structure. Side chains and ATP are drawn in ball-and-stick style. Bonds in ATP are gray. (*A*) Rabbit skeletal muscle α-actin, showing the residues in contact with ATP. (*B*) *Acanthamoeba* Arp2 model with nonidentical residues in black bonds. (*C*) *Acanthamoeba* Arp3, showing residues depicted as in *B*. The side chain for L16F, which is in an identical conformation to L16Y in Arp2, has been omitted to allow visualization of the backbone NH interaction with the β-phosphate of ATP.

Neither Arp antiserum reacts with *Acanthamoeba* actin or with the other Arp.

By quantitative Western blots both Arp2 and Arp3 remain in the supernatant fraction after centrifugation at 100,000 *g* for 90 min (Fig. 7). Arp2 may be slightly depleted from the 100,000 *g* supernatant (one experiment of three, shown in Fig. 7). This may be due to its sedimentation with the profilin-binding complex of *Acanthamoeba*, which has a Stokes' radius of 5.8 nm (Machesky et al., 1994). Arp3 does not seem depleted from the 100,000 *g* supernatant. There is an excess of Arp3 over Arp2, and an excess of each over other members of the profilin-binding complex (Machesky et al., 1994). The Arp2 concentration is 1.9 μM and the Arp3 concentration is 5.1 μM in packed pellets of *Acanthamoeba*.

By indirect immunofluorescence Arp2 is concentrated in the cell cortex (Fig. 8). Pseudopods and cell processes stain intensely. Staining is evident in spikes and lamellae (Fig. 8 *D*). Amoebastomes, cuplike projections of the cell surface which extend and retract on a minute time scale (Doberstein, S. K., I. C. Baines, E. D. Korn, T. D. Pollard, manuscript submitted for publication), label particularly intensely (Fig. 8 *J*). The diffuse labeling of the cytoplasm does not seem to correspond to any subcellular structure. Staining is excluded from the nucleus and other organelles in all cells examined. Faint staining in regions surrounding some, but not all, vacuoles is present in less than 10% of cells examined (Fig. 8 *H*). Mock purified preimmune antiserum does not label fixed amoebas (not shown).

The distribution of Arp2 is very similar to that of filamentous actin stained with BODIPY-FL phallicidin (Fig. 9). Both strongly label an amoebastome in the upper cell pictured in Fig. 9, *B* and *C*. There is no overlap of the rhodamine and fluorescein channels using our filter sets and suppression filters (not shown). Arp3 localization in amoebastomes and the rest of the cell cortex is similar to that of Arp2 and filamentous actin (Fig. 10). Discrete spots of Arp3 staining are evident in the cytoplasm within lamellae. It is not known what structures these correspond to.

Discussion

The determined phylogeny of the Arps and actin is robust based on independent analysis by two different methods. Bootstrapping within each analysis gives a measure of reproducibility. In each case, the placement of the Arps into the groupings shown is well supported by the data. Ambiguities occurred primarily within the actin family, where the degree of identity between pairs of sequences is quite high. The emerging picture based on these phylogenetic analyses (Fyrberg et al., 1994; Michaille et al., 1995; Muhua et al., 1994; Schroer et al., 1994) is that the three major Arp families and conventional actin define a larger class proteins distinct from structurally related ATPases including hexokinase, 70-kD heat shock proteins, and bacterial cell cycle proteins (Bork et al., 1992; Flaherty et al., 1991; Kabsch and Holmes, 1995; Sánchez et al., 1994).

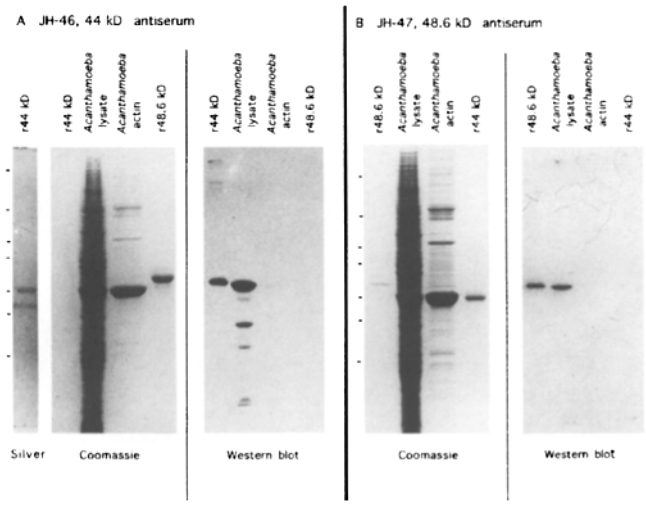

Figure 6. SDS-PAGE of recombinant Arps, *Acanthamoeba* lysate and crude *Acanthamoeba* actin stained with Coomassie blue or Western blotted with polyclonal antiserum against either Arp2 or Arp3. Conditions: proteins were resolved by 10% acrylamide SDS-PAGE. Duplicate gels were either stained with Coomassie blue or transferred to nitrocellulose and reacted with JH-46 antiserum for Arp2 or JH-47 antiserum for Arp3. (*A*) Samples reacted with Arp2 antiserum. The first lane is recombinant Arp2 loaded at the same concentration as in subsequent lanes and silver stained to allow visualization. (*B*) Samples reacted with Arp3 antiserum. Tick marks at left in *A* and *B* indicate molecular weight standards of 200, 95, 68, 60, 43, 40, and 29 kD.

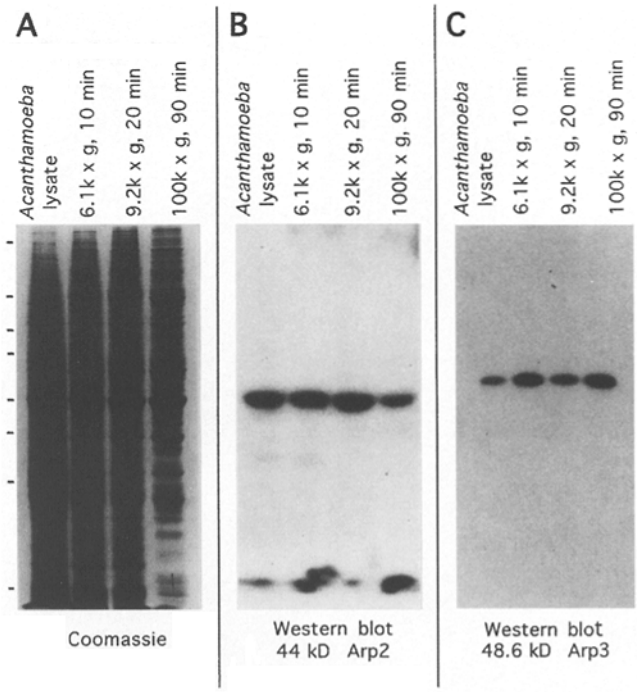

Figure 7. Fractionation of Arp2 and Arp3 during differential centrifugation of *Acanthamoeba* homogenates. The homogenate was centrifuged at 6,100 *g* for 10 min, 9,200 *g* for 20 min and 100,00 *g* for 90 min and the supernatants were run on SDS-PAGE, stained with Coomassie blue or Western blotted with polyclonal antiserum against either Arp2 or Arp3. Conditions: proteins were resolved on 10% acrylamide SDS-PAGE. Duplicate gels were either stained with Coomassie blue or transferred to nitrocellulose and reacted with JH-46 antiserum for Arp2 or JH-47 antiserum for Arp3. Detection is by autoradiography with [^{125}I]protein A. Tick marks at left in *A* indicate molecular weight standards of 200, 95, 68, 60, 43, 40, 29, and 18 kD.

The Arp1, Arp2, and Arp3 families are all represented in and conserved across a wide cross section of eukaryotic species, strongly implying common origins early in eukaryotes and unique biochemical functions for which each has been maintained through evolution. The relationships within the myosin (Goodson and Spudich, 1993) and kinesin superfamilies (Goodson et al., 1994) are similar. Each of these has a unifying set of structural properties, but is subdivided into conserved families with presumed functional differences.

Schwob and Martin (1992) noted the presence of a potential site in ACT2p (residues 49-52, TPLK) for phosphorylation by the mitotic Cdc28/cyclin protein kinase, and postulated that this might contribute to cell cycle control of cytokinesis. However, *S. cerevisiae* ACT2p is the most divergent Arp2 and this sequence is not present in any of the other four Arp2s, which have the sequence I/V E I/V K at the equivalent positions. While we cannot rule out the possibility that this sequence is phosphorylated in yeast ACT2p, this cannot be a general mechanism for the control of Arp2 interactions.

Our method for constructing the structural models given here is intentionally simplistic, essentially overlaying the Arp sequences onto the actin three dimensional structure. Refinement of the models altered the backbone very little. This conservative modeling approach seemed reasonable based upon the pairwise two dimensional alignments of each Arp with actin and highlights many important structural features. The resulting structures should be regarded as models to guide future work. Clearly, the actual structures of these molecules must differ from the models. The insertions, modeled here as loops only constrained by allowed peptide geometry and steric considerations, are likely to fold more compactly than shown in the models, but there is no basis for modeling them differently at present. The regions where insertions occur in the structures may take on new conformations. This seems likely to be the case in subdomain 4 of Arp3, which has an insertion within a region with little homology to actin.

The model structures clearly show that both Arp2 and Arp3 are likely to bind nucleotide and divalent cation. The regions comprising the nucleotide-binding pocket in actin are virtually superimposable on the two model structures. Atoms that ligate calcium, as well as those interacting with the ribose hydroxyls and the phosphates of ATP are all present in geometries nearly identical to actin, and the environment surrounding the adenine moiety is quite similar in actin and both Arp models. Where the residues are not identical, either the change is minor or the backbone NH or CO form the important contacts with the nucleotide.

A complex of proteins containing Arp2 and Arp3 binds profilin (Machesky et al., 1994) so profilin may bind directly to one of the Arps in this complex. The structural models show that Arp2 is much more likely to bind to profilin than Arp3.

The stoichiometry of Arp2 to Arp3 in the profilin-binding complex is 1:1, thus it is possible that the two form a heterodimer within this complex. We compared the Arp models to actin subunits in the Lorenz et al. (1993) model

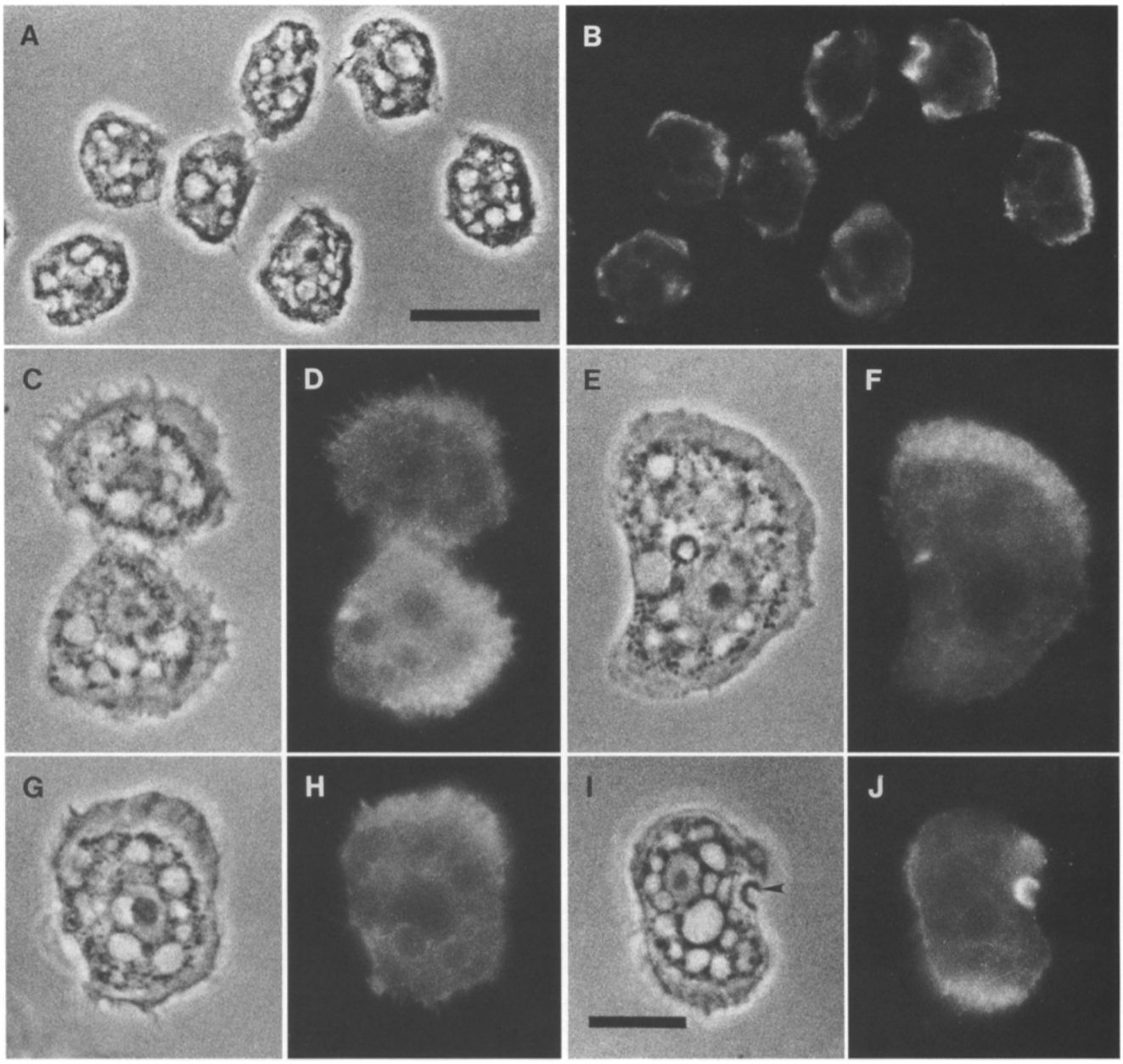

Figure 8. Fluorescence and phase contrast micrographs of *Acanthamoeba* stained with affinity purified polyclonal antiserum to Arp2. (*A, C, E, G,* and *I*) Phase contrast micrographs. (*B, D, F, H,* and *J*) Indirect immunofluorescent labeling of Arp2. Scale in *A* and *B* is 20 μm. Scale in *C–J* is 10 μm. Arrow in *I* points to an amoebastome.

of filamentous actin to explore possible orientations in an Arp2: Arp3 heterodimer. Of the four dimer geometries (Fig. 11), three seem possible from the Arp atomic models. Side chains making long pitch helix interactions are conserved at the barbed ends of both Arp2 and Arp3, partially conserved at the pointed end of Arp2 and absent at the pointed end of Arp3. Therefore, a long pitch dimer with Arp3 at the pointed end and Arp2 at the barbed end (Fig. 11 *B*) is possible, while one with Arp3 at the barbed end is unlikely. Residues which interact across the genetic helix are reasonably conserved in both Arp2 and Arp3; either genetic helix dimer (Fig. 11, *C* and *D*) seems possible. The differences in the Arp2 plug relative to actin may involve interaction with an Arp3 hydrophobic pocket, favoring the genetic helix dimer in Fig. 11, *C* or *D*.

These dimers may be able to interact with actin monomers. Both Arp2 and Arp3 have hydrophobic patches in subdomain 3 which could contribute to a stabilizing hydrophobic pocket like that found in actin. Both Arp2 and Arp3 could potentially provide a hydrophobic plug, although the presence of an aspartic acid in the Arp2 plug may destabilize this interaction. The long pitch Arp dimer with Arp3 at the pointed end has the necessary ligands on Arp2 and Arp3 to bind an actin monomer across the genetic helix and on Arp2 to bind another monomer along the long pitch helix at the barbed end. Actin monomers could bind to the barbed end of this assembly, allowing polymerization in the barbed end direction (Fig. 11 *B*). Either genetic helix Arp dimer has long pitch and genetic helix ligands for actin monomers to bind at the barbed end

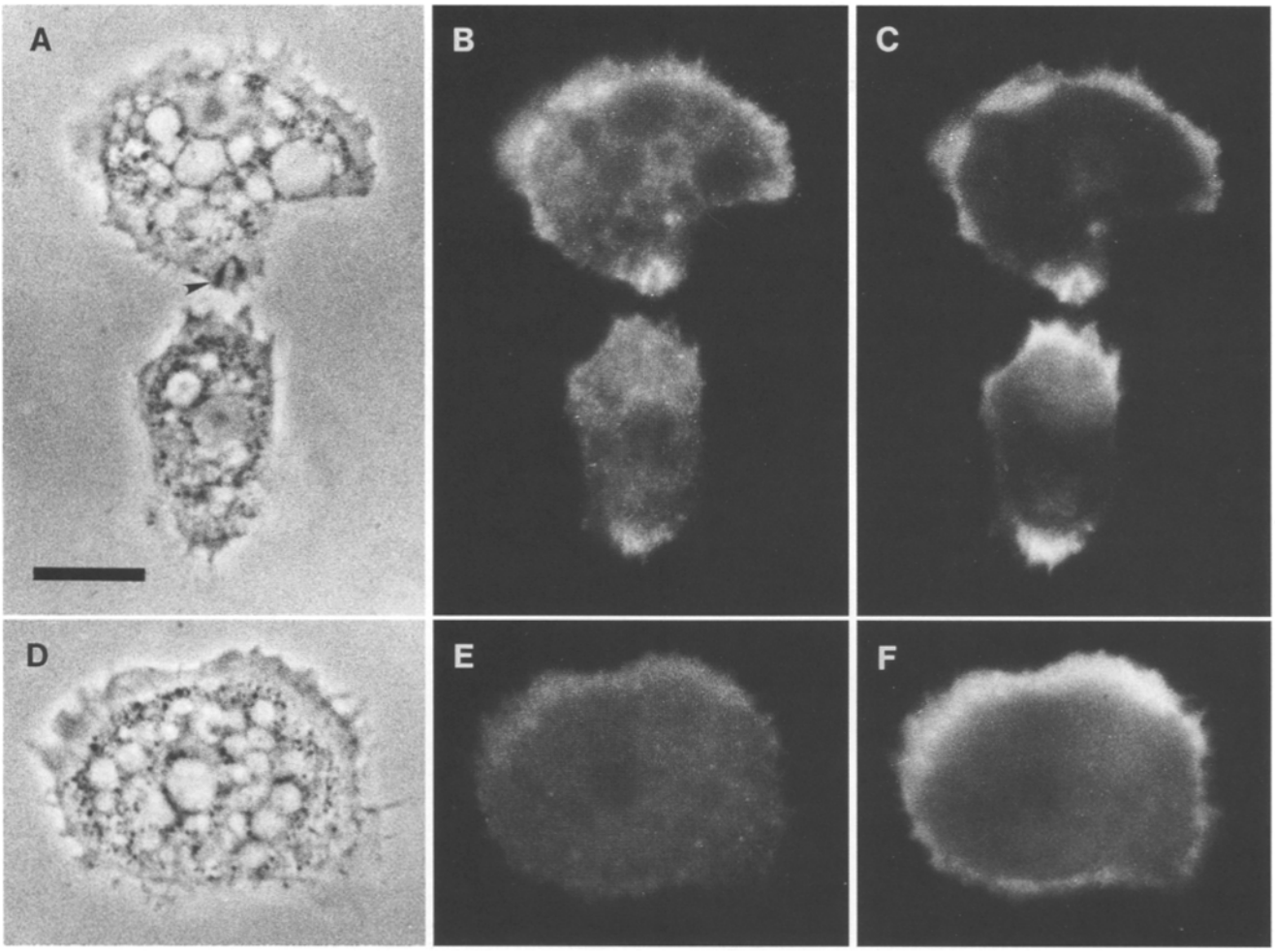

Figure 9. Fluorescence and phase contrast microcrographs of *Acanthamoeba* stained with affinity purified antiserum to Arp2 and BODIPY-FL phallicidin to visualize filamentous actin. (*A* and *D*) Phase contrast micrographs. (*B* and *E*) Indirect immunofluorescent labeling of Arp2. (*C* and *F*) BODIPY-FL phallicidin labeling of filamentous actin. Scale in *A–F* is 10 μm. Arrow in *A* points to an amoebastome.

(Fig. 11, *C* and *D*). The differences at the pointed end of Arp3 relative to actin seem to rule out the possibility of actin filaments nucleating from the pointed end of any of the three likely dimers due to steric interference. An Arp2: Arp3 heterodimer could interact with actin monomers to nucleate barbed end polymerization. One or more of the other polypeptides present in the profilin-binding complex may modulate this interaction.

Yeast actin with the hydrophobic plug mutation L266D, which may be comparable to the Arp2 substitution G267D, displays a cold sensitive polymerization defect, possibly in filament nucleation (Chen et al., 1993). The substitution of a charged residue in the hydrophobic plug of Arp2 may destabilize the interaction with an actin filament growing from an Arp2: Arp3 barbed end nucleus, allowing dissociation of this nucleus once filament polymerization has entered a rapid phase. This might allow an Arp2: Arp3 nucleus to act catalytically.

Other proteins which bind actin may interact with Arp2 or Arp3 at conserved faces. Barbed end interacting proteins of the gelsolin family may be able to bind Arp2 but their binding to Arp3 seems less likely. Pointed end–binding proteins may possibly bind Arp2, but it seems unlikely; they almost certainly do not interact with Arp3.

Given the 40–100-fold excess of actin, Arp2 and Arp3 cannot interact stoichiometrically with actin, but their cellular concentrations (Arp2 = 1.9 μM, Arp3 = 5.1 μM) are comparable to those of other *Acanthamoeba* actin-binding proteins: α-actinin = 4 μM [Pollard et al., 1986]; actophorin = 20 μM [Cooper et al., 1986]; capping protein = ~1.3 μM [Cooper et al., 1984*a*]; and myosin-II = ~1 μM [Kiehart and Pollard, 1984]). The concentration of profilin in *Acanthamoeba* is 100 μM (Tseng et al., 1984).

Arp3 was recently reported to be associated with mitochondria in *D. discoideum* (Murgia et al., 1995). We do not see localization of Arp3 in mitochondria in *Acanthamoeba* with our antibodies nor do we see depletion of significant amounts of Arp3 upon removing mitochondria by centrifugation.

Both Arp2 and Arp3 are strongly enriched in the cortex of *Acanthamoeba*, as observed for filamentous actin in this and previous studies (Yonemura and Pollard, 1992). Several models of amoeboid motility feature dynamic actin filaments in the cortex, with rapid turnover of the G- and

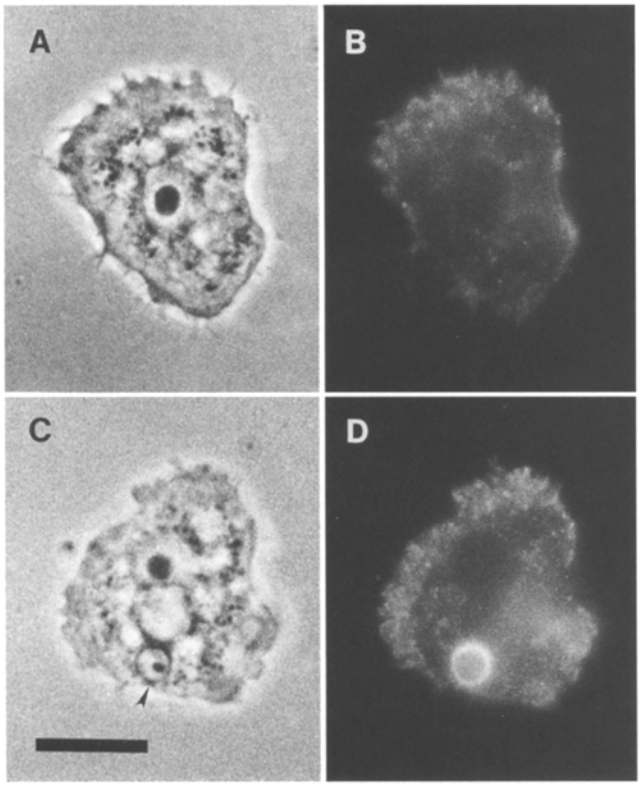

Figure 10. Fluorescence and phase micrographs of *Acanthamoeba* stained with affinity purified polyclonal antiserum to Arp3. (*A* and *C*) Phase contrast micrographs. (*B* and *D*) Indirect immunofluorescent labeling of Arp3. Scale in *A–D* is 10 μm. Arrow in *C* points to an amoebastome.

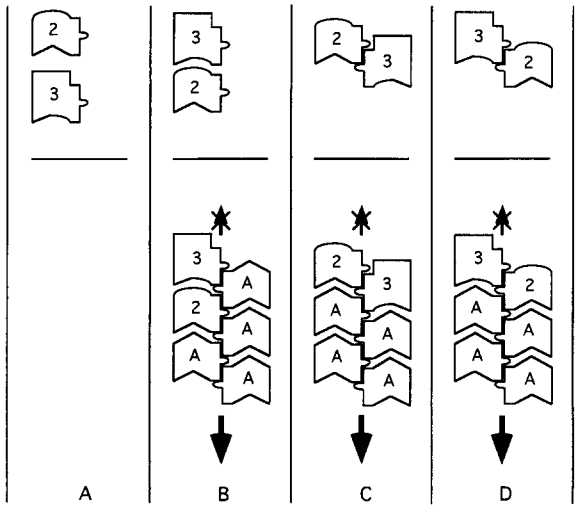

Figure 11. Schematic representation of possible Arp2: Arp3 dimers and their potential interactions with actin monomers. Arp2 is labeled 2. Arp3 is labeled 3. Actin is labeled A. Dimers are shown at the top of each column, interactions with actin are below. The pointed end is toward the top of the page. The barbed end is toward the bottom of the page. Arrows in *B–D* indicate actin filament polymerization.

F- actin pools, polymerization at the leading edge, and depolymerization elsewhere (Condeelis, 1993; Cooper, 1991; Theriot and Mitchison, 1991). Nucleation of actin filaments from free monomers is the rate limiting step in spontaneous actin polymerization (Pollard and Cooper, 1986). The structure of Arp2 and Arp3 and their coexistence in a stable complex concentrated in the cortex suggests that these Arps may play some role in the actin dynamics in this region, perhaps as a nucleus in the context of the profilin-binding complex, promoting filament assembly in the barbed end direction.

We are grateful to Dr. A. Gittis for help with building the molecular models, Dr. H. Goodson for advice on phylogenetic analysis, Dr. J. Duwve for assistance with constructing the *Acanthamoeba* cDNA library, I. Goldberg for technical advice and members of the Pollard lab for technical advice and helpful discussion.

This work was supported by National Institutes of Health Research grant GM-26338 to T. D. Pollard and GM-35171 to E. E. Lattman and T. D. Pollard.

Received for publication 11 May 1995 and in revised form 11 July 1995.

References

Bork, P., C. Sander, and A. Valencia. 1992. An ATPase domain common to prokaryotic cell cycle proteins, sugar kinases, actin, and hsp70 heat shock proteins. *Proc. Natl. Acad. Sci. USA.* 89:7290–7294.

Brünger, A.T. 1992. X-PLOR Version 3.1 a system for X-ray crystallography and NMR. Yale University Press, New Haven.

Chen, X., K. Cook, and P. A. Rubenstein. 1993. Yeast actin with a mutation in the "hydrophobic plug" between subdomains 3 and 4 (L_{266}D) displays a cold-sensitive polymerization defect. *J. Cell Biol.* 123:1185–1195.

Clark, S. W., and D. I. Meyer. 1992. Centractin is an actin homologue associated with the centrosome. *Nature (Lond.).* 359:246–250.

Clark, S. W., and D. I. Meyer. 1993. Long lost cousins of actin. *Curr. Biol.* 3:54–55.

Clark, S. W., and D. I. Meyer. 1994. *ACT3*:a putative centractin homologue in *S. cerevisiae* is required for proper orientation of the mitotic spindle. *J. Cell Biol.* 127:129–138.

Clark, S.W., O. Staub, I. Clark, E. L. F. Holzbaur, B. M. Paschal, R. B. Vallee, and D. I. Meyer. 1994. β-Centractin: characterization and distribution of a new member of the centractin family of actin-related proteins. *Mol. Biol. Cell.* 5:1301–1310.

Condeelis, J. 1993. Life at the leading edge: the formation of cell protrusions. *Annu. Rev. Cell Biol.* 9:411–444.

Cooper, J. A. 1991. The role of actin polymerization in cell motility. *Annu. Rev. Physiol.* 53:585–605.

Cooper, J. A., J. D. Blum, and T. D. Pollard. 1984*a*. *Acanthamoeba castellanii* capping protein: properties, mechanism of action, immunologic cross-reactivity, and localization. *J. Cell Biol.* 99:217–225.

Cooper, J. A., J. D. Blum, R. C. Williams, and T. D. Pollard. 1986. Purification and characterization of actophorin, a new 15,000 dalton actin binding protein from *Acanthamoeba castellanii*. *J. Biol. Chem.* 261:477–485.

Evans, S. V. 1993. SETOR: hardware lighted three-dimensional solid model representations of macromolecules. *J. Mol. Graphics.* 11:134–138.

Felsenstein, J. 1985. Confidence limits on phylogenies: an approach using the bootstrap. *Evolution.* 39:783–791.

Flaherty, K. M., D. B. McKay, W. Kabsch, and K. C. Holmes. 1991. Similarity of the 3-dimensional structures of actin and the ATPase fragment of a 70-kD heat-shock cognate protein. *Proc. Natl. Acad. Sci. USA.* 88.5041–5045.

Frankel, S., M. B. Heintzel, S. Artavani, and M. S. Mooseker. 1994. Identification of a divergent actin-related protein in drosophila. *J. Mol. Biol.* 235: 1351–1356.

Fujiwara, K., and T. D. Pollard. 1976. Fluorescent antibody localization of myosin in the cytoplasm, cleavage furrow, and mitotic spindle of human cells. *J. Cell Biol.* 71:848–875.

Fyrberg, C., L. Ryan, M. Kenton, and E. Fyrberg. 1994. Genes encoding actin-related proteins of *Drosophila*. *J. Mol. Biol.* 241:498–503.

Goodson, H. V., and J. A. Spudich. 1993. Molecular evolution of the myosin family: relationships derived from comparisons of amino acid sequences. *Proc. Natl. Acad. Sci. USA.* 90:659–663.

Goodson, H. V., S. J. Kang, and S. A. Endow. 1994. Molecular phylogeny of the kinesin family of microtubule motor proteins. *J. Cell. Sci.* 107:1875–1884.

Hammer, J. A., B. Bowers, B. M. Paterson, and E. D. Korn. 1987. Complete nucleotide-sequence and deduced polypeptide sequence of a nonmuscle myosin heavy-chain gene from *Acanthamoeba*—evidence of a hinge in the rod-like tail. *J. Cell Biol.* 105:913–925.

Harata, M., A. Karwan, and U. Wintersberger. 1994. An essential gene of *Sac-*

charomyces cerevisiae coding for an actin-related protein. *Proc. Natl. Acad. Sci. USA.* 91:8258–8262.

Higgins, D. G., A. J. Bleasby, and R. Fuchs. 1992. Clustal V: improved software for mutiple sequence alignment. *CABIOS.* 8:189–191.

Hightower, R. C., and R. B. Meagher. 1986. The molecular evolution of actin. *Genetics.* 114:315–332.

Kabsch, W., and K. C. Holmes. 1995. The actin fold. *FASEB (Fed. Am. Soc. Exp. Biochem.) J.* 9:167–174.

Kabsch, W., H. G. Mannherz, D. Suck, E. Pai, and K. C. Holmes. 1990. Atomic structure of the actin:DNase I complex. *Nature (Lond.).* 347:37–44.

Kimura, M. 1983. The Neutral Theory of Molecular Evolution. Cambridge University Press, Cambridge, England. 367 pp.

Kiehart, D. P., and T. D. Pollard, 1984. Inhibition of *Acanthamoeba* actomyosin-II ATPase activity and mechanochemical function by specific monoclonal antibodies. *J. Cell Biol.* 99:1024–1033.

Kraulis, P. 1991. MOLSCRIPT: a program to produce both detailed and schematic plots of protein structures. *J. Appl. Crystal.* 24:946–950.

Laemmli, U. K. 1970. Cleavage of structural proteins during the assembly of the head of bacteriophage T4. *Nature (Lond.).* 227:680–685.

Lees-Miller, J. P., D. M. Helfman,and T. A. Schroer. 1992*a*. A vertebrate actin-related protein is a component of a multisubunit complex involved in microtubule-based vesicle motility. *Nature(Lond.).* 359:244–246.

Lees-Miller, J. P., G. Henry, and D. M. Helfman. 1992*b*. Identification of *act2*, an essential gene in the fission yeast *Schizosaccharomyces pombe* that encodes a protein related to actin. *Proc. Natl. Acad. Sci. USA.* 89:80–83.

Lorenz, M., D. Popp, and K.C. Holmes. 1993. Refinement of the F-actin model against x-ray fiber diffraction data by the use of a directed mutation algorithm. *J. Mol. Biol.* 234:826–836.

Machesky, L. M., S. J. Atkinson, C. Ampe, J. Vandekerckhove, and T. D. Pollard. 1994. Purification of a cortical complex containing two unconventional actins from *Acanthamoeba* by affinity chromatography on profilin agarose. *J.Cell Biol.* 127:107–115.

Machesky, L. M., and T. D. Pollard. 1993. Profilin as a potential mediator of membrane cytoskeletal communication. *Trends Cell Biol.* 3:381–385.

Melki, R., I. E. Vainberg, R. L. Chow, and N. J. Cowan. 1993. Chaperonin-mediated folding of vertebrate actin-related protein and γ-tubulin. *J. Cell Biol.* 122:1301–1310.

Michaille, J., M. Gouy, S. Blanchet, and L. Duret. 1995. Isolation and characterization of a cDNA encoding a chicken actin-like protein. *Gene (Amst).* 154: 205–209.

Murgia, I., S. K. Maciver, and P. Morandini. 1995. An actin-related protein from *Dictyostelium discoideum* is developmentally regulated and associated with mitochondria. *FEBS Lett.* 360:235–241.

Muhua, L., T. S. Karpova, and J. A. Cooper. 1994. A yeast actin-related protein homologous to that in vertebrate dynactin complex is important for spindle orientation and nuclear migration. *Cell.* 78:669–679.

Nagai, K., and Thøgersen, H.C. 1987. Synthesis and sequence-specific proteolysis of hybrid proteins produced in *Escherichia coli. Methods Enzymol.* 153: 461–481.

Paschal, B. M., E. L. F. Holzbaur, K. K. Pfister, S. Clark, D. I. Meyer, and R. B. Vallee. 1993. Characterization of a 50-kDa polypeptide in cytoplasmic dynein preparations reveals a complex with p150GLUED and a novel actin. *J. Biol. Chem.* 268:15318–15323.

Plamann, M., P. F. Minke, J. H. Tinsley, and K. S. Bruno. 1994. Cytoplasmic dynein and actin-related protein Arp1 are required for normal nuclear distribution in filamentous fungi. *J. Cell Biol.* 127:139–141.

Pollard, T. D. 1984. Purification of a high molecular-weight actin filament gelation protein from *Acanthamoeba* that shares antigenic determinants with vertebate spectrins. *J. Cell Biol.* 99:1970–1980.

Pollard, T. D., and J. A. Cooper. 1986. Actin and actin-binding proteins. A critical evaluation of mechanisms and functions. *Annu. Rev. Biochem.* 55:987–1035.

Pollard, T. D., P. C.-H. Tseng, D. L. Rimm, D. P. Bichell, R. C. Williams, and J. Sinard. 1986. Characterization of alpha-actinin from *Acanthamoeba. Cell Motil.* 6:649–661.

Saitou, N., and M. Nei. 1987. The neighbor-joining method: a new method for reconstructing phylogenetic trees. *Mol. Biol. Evol.* 4:406–425.

Sambrook, J., E. F. Fritsch, and T. Maniatis. 1989. Molecular Cloning: A Laboratory Manual. Cold Spring Harbor Laboratory Press, Cold Spring Harbor, NY.

Sánchez, M., A. Valencia, M. Ferrándiz, C. Sander, and M. Vicente. 1994. Correlation between the structure and biochemical activities of FtsA, an essential cell division protein of the actin family. *EMBO(Eur. Mol. Biol. Organ.) J.* 13:4919–4925.

Schafer, D. A., S. R. Gill, J. A. Cooper, J. E. Heuser, and T. A. Schroer. 1994. Ultrastructural analysis of the dynactin complex: an actin-related protein is a component of a filament that resembles actin. *J. Cell Biol.* 126:403–412.

Schroer, T., E. Fyrberg, J. Cooper, R. Waterston, D. Helfman, T. Pollard, and D. Meyer. 1994. Actin-related protein nomenclature and classification. *J. Cell Biol.* 127:1777–1778.

Schroer, T. A. 1994. New insights into the interaction of cytoplasmic dynein with the actin-related protein, Arp1. *J. Cell Biol.* 127:1–4.

Schutt, C., J. C. Myslik, M. D. Rozychi, N. C. W. Goonesekere, and U. Lindberg. 1993. The structure of crystalline profilin-β-actin. *Nature (Lond.).* 365: 810–816.

Schwob, E., and R. P. Martin. 1992. New yeast actin-like gene required late in the cell cycle. *Nature (Lond.).* 355:179–182.

Tanaka, T., F. Shibasaki, M. Ishikawa, N. Hirano, R. Sakai, J. Nishida, T. Takenawa, and H. Hirai. 1992. Molecular cloning of bovine actin-like protein, actin2. *Biochem. Biophys. Res. Commun.* 187:1022–1028.

Theriot, J. A., and T. J. Mitchison. 1991. Actin microfilament dynamics in locomoting cells. *Nature (Lond.).* 352:126–131.

Theriot, J. A., and T. J. Mitchison. 1993. The three faces of profilin. *Cell.* 75: 835–838.

Towbin, H., T. Stahelin, and J. Gordon. 1979. Electrophoretic transfer of proteins from polyacrylamide gels to nitrocellulose sheets: procedures and some applications. *Proc. Natl. Acad. Sci. USA.* 76:4350–4354.

Tseng, P. C. H., M. S. Runge, J. A. Cooper, R. C. Williams, Jr., and T. D. Pollard. 1984. Physical, immunochemical, and functional properties of *Acanthamoeba* profilin. *J. Cell Biol.* 98:214–221.

Waterston, R., C. Martin, M. Craxton, C. Huynh, A. Coulson, L. Hillier, R. Durbin, P. Green, R. Shownkeen, N. Halloran, et al. 1992. A survey of expressed genes in *Caenorhabditis elegans. Nat. Genet.* 1:114–123.

Way, M., B. Pope, J. Gooch, M. Hawkins, and A. G. Weeds. 1990. Identification of a region in segment 1 of gelsolin critical for actin binding. *EMBO (Eur. Mol. Biol. Organ.) J.* 9:4103–4109.

Yonemura, S. Y., and T. D. Pollard. 1992. Localization of myosin-I and myosin-II in *Acanthamoeba. J. Cell Sci.* 102:629–642.